Journal of Catalysis 301 (2013) 46–53

Contents lists available at SciVerse ScienceDirect

Journal of Catalysis

journal homepage: www.elsevier.com/locate/jcat

Microstructured Au/Ni-fiber catalyst: Galvanic reaction preparation and catalytic performance for low-temperature gas-phase alcohol oxidation

Guofeng Zhao [a], Miaomiao Deng [a], Yifeng Jiang [a], Huanyun Hu [a], Jun Huang [b], Yong Lu [a,*]

[a] Shanghai Key Laboratory of Green Chemistry and Chemical Processes, Department of Chemistry, East China Normal University, Shanghai 200062, China
[b] School of Chemical and Biomolecular Engineering, University of Sydney, NSW 2006, Australia

ARTICLE INFO

Article history:
Received 4 December 2012
Revised 24 January 2013
Accepted 25 January 2013

Keywords:
Gold catalyst
Nickel fiber
Galvanic deposition
Alcohol oxidation
Aldehyde

ABSTRACT

The highly active and selective gold catalysts were successfully prepared by galvanically depositing Au onto a thin-sheet microfibrous structure consisting of 5 vol.% 8-μm Ni-fiber and 95 vol.% voidage, with high heat conductivity and good stability for the gas-phase oxidation of alcohols. The best catalyst was Au-4/Ni-fiber-300 (Au-loading: 4 wt%; calcined at 300 °C in air), being effective for oxidizing acyclic, benzylic, and polynary (1,2-propanediol) alcohols. For benzyl alcohol, the conversion of 95% was achieved with 99% selectivity to benzaldehyde within 660 h test at 250 °C, while a low ΔT of <10 °C between catalyst bed and reactor external wall was observed. Transformation of $NiCl_2$ formed at Au galvanic deposition step into NiO was identified along with the low-temperature activity promotion. This suggests a special synergistic effect between NiO and Au particles, of which comprehensive understanding is particularly desirable.

1. Introduction

The selective oxidation of alcohols to the corresponding carbonyl compounds is one of the most important processes in the synthesis of fine chemicals and pharmaceuticals such as vitamins and fragrances [1–4]. However, the use of various toxic and expensive stoichiometric inorganic oxidants and volatile organic solvents in the existing oxidation processes causes serious problems in product separation and environmental issues, obviously conflicting the atom-economical concept of green chemistry [5–9]. Thus, there is an urgent need to develop cleaner selective oxidation processes, aimed at using atmospheric air and recyclable heterogeneous catalysts under solvent-free conditions [1–3].

The catalytic aerobic oxidation of alcohols has been extensively investigated in the liquid phase based on homogeneous catalysts [3,10,11] and supported noble metals (Pd-, Au-, or Ru-based) [1,2,4,12]. The high selectivity has been obtained on those catalysts; however, the reaction processes suffer from low reaction rate, high O_2 pressure, and catalyst/solvent separation issues. From the industrial point of view, the gas-phase oxidation of alcohols would be a promising route because of the easy catalyst separation, solvent-free process, and much higher production efficiency [1,2]. However, further industrial application still remains particularly challenging. Because of the strong exothermicity of the gas-phase alcohol oxidation, it is desirable to endow the catalyst with good heat conductivity for rapidly dissipating reaction heat from catalyst bed. On the other hand, it is also desirable to endue the catalyst with good low-temperature activity for suppressing the thermal cracking and over oxidation of the alcohols (especially the large molecules).

However, the catalysts with good heat conductivity reported so far generally showed the poor low-temperature activity and required high reaction temperatures (e.g., >350 °C) to achieve an acceptable conversion with low selectivity due to thermal cracking and overoxidation [13]. For example, commercial electrolytic bulk silver catalyst utilized in methanol oxidation to formaldehyde is characteristic of excellent heat conductivity but becomes active only at above 500 °C for the large alcohol molecules, such as benzyl alcohol [14,15]. Reversely, the oxide-supported Au [16,17], Cu [18,19], and Ag [20] catalysts demonstrated good low-temperature activity, but their weak heat conductivity easily induces hotspots in the reaction bed [17,18]. In the gas-phase oxidation of benzyl alcohol, a large bed temperature increase of ~56 °C was reported over Au–Cu/SiO_2 (0.2 g) [17] using a weight hourly space velocity (WHSV) of 10 h^{-1}, as well as ~17 °C over K–Cu–TiO_2 (0.2 g) [18] even using a very small WHSV of 0.6 h^{-1}. It causes not only the catalyst degradation but also a hidden danger (e.g., catalyst bed temperature out of control), which limits their industrial application.

Hence, for both academic research and industrial application, a challenge of the catalyst for the gas-phase alcohol oxidation is how to well combine the high heat conductivity with excellent low-temperature activity. One attractive solution is to apply the highly heat-conductive supports for active nano-catalyst. Silver catalyst

* Corresponding author. Fax: +86 21 62233424.
E-mail address: ylu@chem.ecnu.edu.cn (Y. Lu).

0021-9517/$ - see front matter © 2013 Elsevier Inc. All rights reserved.
http://dx.doi.org/10.1016/j.jcat.2013.01.020

supported on the LTA zeolite film coated on a copper grid has been reported to show good low-temperature activity and high selectivity for the gas-phase oxidation of benzyl alcohol [13]. Recently, a new class of paper-like sintered-metal-microfiber (SMF) has been used as an ideal support, due to its three-dimensional network, open structure, and extremely high heat conductivity [14,15,21–31]. Such microfibrous structure with unique form factors can be made into thin sheets (from submillimeter to several millimeters in thickness) of large area and/or pleated sheet structure to control pressure drop and contacting efficiency in a beneficial manner different from other traditionally employed contacting schemes including packed beds, honeycomb monoliths or wovens, and grid [14,15,21–31]. Therefore, this microfibrous material is a promising support for hosting high-performance nano-catalysts, especially for the strongly endothermic and exothermic reactions. Our previous efforts have successfully applied this microfibrous support in the NH_3 cracking [22–24], methanol steam reforming [25], H_2 fuel cleanup (CO and H_2S removal) [28], O_3 catalytic decomposition [29], methane dry reforming [30,31] and more recently, the gas-phase oxidation of alcohols over microfibrous-structured Ag [14,15,26] and Au [27,32,33] catalysts.

In order to combine the low-temperature activity of Au NPs and the excellent heat conductivity of metallic microfibrous supports, we developed a new-type microfibrous-structured Au/Ni-fiber catalyst in this research. Similar with the preparation method of the reported catalysts such as Au/Ag [34] and Au/Pd [35], our Au/Ni-fiber catalyst was prepared with the aid of galvanic exchange reaction between $HAuCl_4$ and Ni-microfiber ($3Ni + 2HAuCl_4 = 2Au + 3NiCl_2 + 2HCl$). The resulting Au/Ni-fiber catalysts from this emerging galvanic deposition were active, selective, and stable for the gas-phase oxidation of alcohols under mild conditions while showing high heat-transfer ability. The formation of NiO@Au ensembles (i.e., transformed from $NiCl_2$@Au composites during the reaction) on the Ni-fiber was clearly identified and contributed to the low-temperature activity. The effects of the catalyst preparation and reaction conditions on the catalyst performance were also investigated, as well as its heat conductivity, the oxidation for a series of alcohols, and the stability.

2. Experimental

2.1. Catalyst preparation

Sinter-locked three-dimensional (3D) SMF networks consisting of 5 vol.% 8-μm-Ni microfibers (Western Metal Material Co., Ltd., China) and 95 vol.% voidage were built up by the regular papermaking/sintering processes [14,15,21–26]. A typical procedure is as follows: Ni-fiber chops with 3–4 mm length (5 g) and cellulose fibers (1.5 g) were added into water (1 L) and stirred vigorously to produce a uniform suspension. The resulting suspension was transferred into the head box of a 159-mm-diameter circular sheet former (ZCX-159A, China), and a circular preform was then formed by draining and drying in air. As-made preform paper was oxidized in air at 300 °C to remove the cellulosic binders and subsequently sintered in hydrogen at 900 °C to create the 3D sinter-locked networks. Gold was then deposited on this sinter-locked Ni-fiber with the aid of galvanic exchange reaction. This process could proceed automatically at room temperature when incipiently impregnating such Ni-fiber carrier with an aqueous solution containing appointed amount of $HAuCl_4$. The resulting samples were dried overnight at 80 °C and calcined in air at temperature range between 200 and 400 °C for 4 h to obtain Au/Ni-fiber catalysts (called as-prepared catalysts). The obtained catalysts were labeled as Au-x/Ni-fiber-y, where "x" denotes Au-loading and "y" denotes the calcination temperatures in air. The Ti-fiber (16 μm dia.; IntraMicron, Ltd., USA) and 316 L stainless steel fiber (8 μm dia.; Western Metal Material Co., Ltd., China) were also used as supports to prepare the Au catalysts for comparative studies.

2.2. Catalyst characterizations

The catalysts were characterized by scanning electron microscopy (SEM, Hitachi S-4800), X-ray diffraction (XRD, Rigaku Uitima IV diffractometer (Cu Kα)), and transmission electron microscopy (TEM, JEOL-JEM-2010 instrument at 200 kV). Specific surface area was determined from N_2 adsorption isotherm at −196 °C using standard Brunauer–Emmett–Teller (BET) theory. X-ray photoelectron spectroscopy (XPS) was recorded on a VG EscaLab 220i spectrometer, using a standard Al Kα X-ray source (300 W) and an analyzer pass energy of 20 eV. All binding energies are referenced to the adventitious C1s line at 284.9 eV. Gold loading of the typical Au-4/Ni-fiber-300 (Au-loading: 4 wt%; calcined at 300 °C in air) sample was determined to be 3.8 wt% by inductively coupled plasma atomic emission spectrometry (ICP-AES) on a Thermo Scientific iCAP 6300 ICP spectrometer.

2.3. Reactivity tests

The gas-phase selective oxidation of alcohols on these catalysts with molecular oxygen was carried out on a fixed-bed quartz tube reactor (i.d., 16 mm) under atmospheric pressure as described previously [14,15,26,27]. Circular chips (16.1 mm diameter) of the microfibrous-structured Au/Ni-fiber catalysts were punched down from their large sheet sample and packed layer-up-layer into the tube reactor with total mass of 0.3 g. Note that the diameter of 0.1 mm larger than the i.d. of the tubular reactor was retained deliberately to avoid the appearance of the gap between the reactor wall and the edges of the catalyst chips thereby preventing the gas bypassing. Alcohols were fed continuously using a high-performance liquid pump, in parallel with O_2 (oxidant) and N_2 (diluted gas) feeding using the calibrated mass flow controllers, into the reactor heated to the desired reaction temperature. The organic phase of the liquid effluent was collected for analyzing by an HP 5890 gas chromatography–flame ionization detector (GC–FID) with a 60-m HP-5 ms capillary column. The gas-phase products such as H_2, CO_x, and C1–C3 hydrocarbons were analyzed by an HP-5890 GC with thermal conductivity detector (TCD) and a 30-m AT-plot 300 capillary column. Reaction temperature, WHSV, and alcoholic hydroxyl (O_2/ol) were varied in range from 220 to 380 °C, 10 to 70 h^{-1}, and 0.4 to 1.2, respectively. Prior to the reaction testing, as-prepared catalysts were all activated by performing the benzyl alcohol oxidation at a high temperature of 380 °C for 1 h, using molar ratio of O_2 to O_2/ol = 0.6 and WHSV = 20 h^{-1}.

3. Results and discussion

3.1. Microfibrous structure, surface morphology, and gold galvanic deposition

Fig. 1 shows the microstructure, surface morphology of the Ni-microfibrous structure before and after the galvanic exchange reaction during Au depositing. A typical SMF-Ni support was prepared by regular wet layup papermaking with a subsequent sintering process, which is characteristic of irregular 3D microfibrous networks (Fig. 1A) and a flexible thin-sheet structure (Fig. 1B). Such microfibrous structure consisted of 5 vol.% of 8-μm Ni-fiber and 95 vol.% of voidage, with a N_2-BET surface area of ~0.6 m^2/g, and fiber surface composited of metallic Ni (dominant) and NiO (Fig. S1). Gold was then successfully and firmly anchored onto the Ni-fiber surfaces with the aid of a simple galvanic exchange

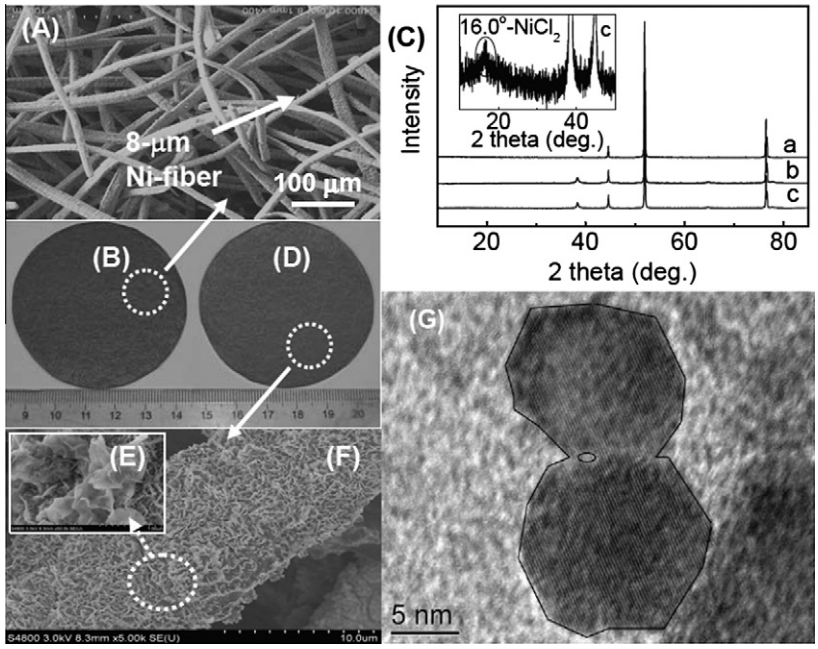

Fig. 1. Microfibrous structure, surface morphology, and XRD patterns of the pure monolithic sinter-locked Ni-fiber and the as-prepared Au-4/Ni-fiber-300 catalyst. (A) Three-dimensional microfibrous structure and surface morphology of the sinter-locked 8-μm Ni-fiber; (B) optical photograph of the large-area structure of sinter-locked Ni-fiber; (C) XRD patterns of the pure Ni-fiber (a), the Au-4/Ni-fiber (gold loading of 4 wt%) just after undergoing Au galvanic deposition without drying (b) and then after calcining at 300 °C in air for 2 h (obtaining as-prepared Au-4/Ni-fiber-300 catalyst) (c); (D) optical photograph, (E and F) SEM and (G) TEM images of the as-prepared Au-4/Ni-fiber-300 catalyst.

reaction deposition method (denoted as galvanic deposition) [27,34,35].

For the confirmation of galvanic deposition, a representative Au-4/Ni-fiber sample (Au-loading of 4 wt%; without calcination treatment) was investigated by XRD as shown in Fig. 1C (with the detailed information in Fig. S2). The pure sinter-locked Ni-fiber was used as a reference in Fig. 1C (pattern a). As the sinter-locked Ni-fiber support was exposed to $HAuCl_4$ aqueous solution, a new peak at 38.2° was observed in Fig. 1C (pattern b) due to the formation of gold particles. It means that the galvanic exchange reaction between $HAuCl_4$ and Ni-fiber proceeded automatically to generate Au particles on Ni surface. The driving force for such gold galvanic deposition comes from the large difference in electrode potential between Ni^{2+}/Ni^0 (−0.25 V) and Au^{3+}/Au^0 (1.5 V) pairs. After drying and calcining at 300 °C in air for 2 h, a representative as-prepared catalyst (Au-4/Ni-fiber-300: gold loading of 4 wt% and calcination temperature of 300 °C) was obtained. The XRD pattern (Fig. 1C, pattern c) shows that $NiCl_2$ (2θ: 16°) was formed on the as-prepared catalyst. This was confirmed by XPS analyses that the catalyst surface has been covered by the dominant $NiCl_2$ (Ni^{2+}: 856.5 eV [36]) and metallic Au species (Au^0: 84 eV [37,38]) (Fig. S3; Scheme S1). A few of NiO (Ni^{2+}: 854.4 eV [36]) and cationic Au (Au^+: 84.8 eV, Au^{3+}: 86.1 eV [37,38]) were also found on the as-prepared catalyst surface. However, no metallic Ni (852.5 eV [36]) was detected, indicating a complete coverage of Ni-fiber surface with the Au species and $NiCl_2$.

An optical photograph of the Au-4/Ni-fiber-300 catalyst (Fig. 1D) shows a well-preserved thin-sheet structure. Such thin-sheet microfibrous-structured gold catalyst can be cut into small pieces (such as circle disk) or made into pleated sheet, demonstrating its robustness and unique form factor for advanced design of reactor [14,15,22–27]. In comparison with the smooth surface of Ni-fiber in Fig. 1A, the Au-4/Ni-fiber-300 catalyst provided uniform $NiCl_2$@Au composites (indicated by XRD results in Fig. 1C and XPS results in Fig. S3) on the Ni-fiber (Fig. 1E and F) after gold galvanic deposition, with the increased surface area from 0.6 m^2/g-fiber to 4.5 m^2/g-cat. TEM image (Fig. 1G) of the Au-4/Ni-fiber-300 shows that Au particles exhibited rough perimeter and uneven contrast features rather than semi-spherical or spherical structures, and the lamellar-shape of gold particles was produced from the Au–Ni galvanic exchange reaction. Au particle size was estimated to be 20–30 nm from both the Scherrer equation according to Au(1 1 1) XRD peak and TEM observation, larger than that for most oxide-supported gold catalysts [4,12,38–46].

3.2. Gas-phase oxidation of benzyl alcohol over Au/Ni-fiber

3.2.1. Effects of Au-loading, calcination temperature, and pre-activation

Firstly, the as-prepared Au/Ni-fiber catalysts with various Au-loadings after calcining at different temperatures were all examined directly in the oxidation of benzyl alcohol at 280 °C using a WHSV of 20 h^{-1} and O_2/ol of 0.6, and the results was shown in Figs. 2A and B. Both Au-loading and calcination temperature have clear influence on the catalytic performance. Increasing the Au-loading from 1 to 4 wt% significantly boosted the conversion from 11% to 84%. Continuously increasing the Au-loading to 6 wt% almost made no impact on the selectivity but slightly increased the conversion to 89%. For the Au-4/Ni-fiber catalysts, benzyl alcohol conversion remarkably enhanced from 36% to 85% when the calcination temperature was increased from 200 to 300 °C. However, a further increase in the calcination temperatures decreased the reactivity slightly (Fig. 2B).

An interesting observation was that activity of the Au/Ni-fiber catalysts for the gas-phase oxidation of benzyl alcohol was promoted dramatically after undergoing 1 h reaction at 380 °C in advance (called pre-activation, using WHSV = 20 h^{-1} and O_2/ol = 0.6). In detail, the catalysts with various Au-loadings were all calcined at 300 °C and then pre-activated at 380 °C for 1 h prior to oxidation of benzyl alcohol at 280 °C. Figs. 2C and D show the conversion and selectivity for all the catalysts after pre-activation.

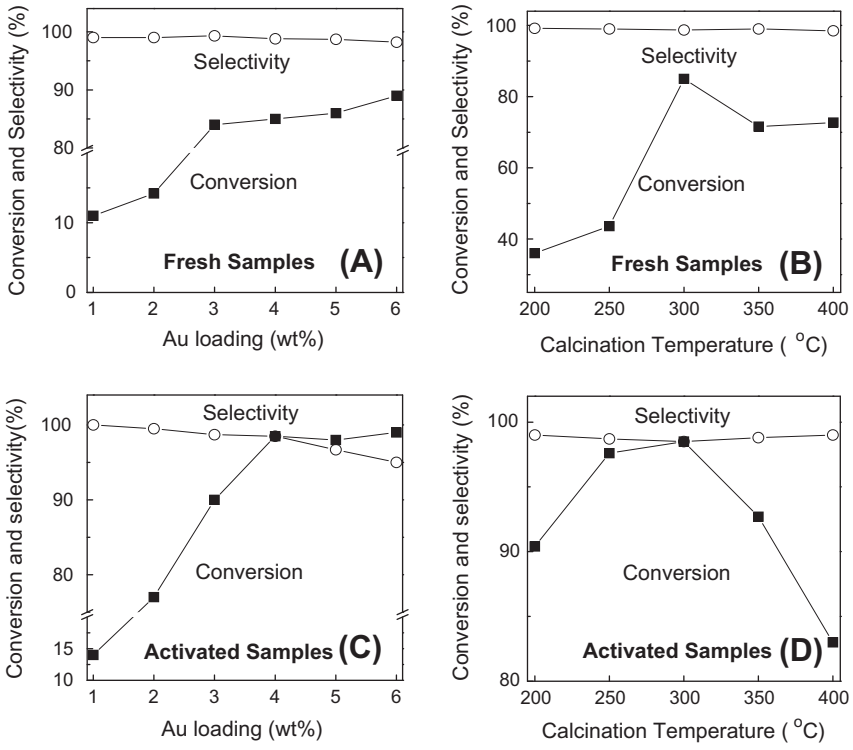

Fig. 2. Effects of the catalyst preparation parameters on the performance of Au/Ni-fiber catalysts for the gas-phase oxidation of benzyl alcohol at 280 °C using O_2/ol of 0.6 and WHSV of 20 h^{-1}. (A and C) Au-loading; (B and D) catalyst calcination temperature. As-prepared samples: as-prepared catalysts just after calcining; Pre-activated samples: the as-prepared catalysts underwent 1 h reaction in the gas-phase oxidation of benzyl alcohol at 380 °C with O_2/ol = 0.6 and WHSV = 20 h^{-1}, prior to the tests at low temperatures.

In comparison with the results shown in Figs. 2A and B, it is noticeable that the low-temperature activity of all the Au/Ni-fiber catalysts for the gas-phase oxidation of benzyl alcohol was dramatically promoted after pre-activation. It is clear from Fig. 2C that the benzyl alcohol conversion was not linearly increased with gold loading from 1 to 4 wt%. Therefore, the high activity of the Au-4/Ni-fiber catalyst is from not only a high gold loading, but also another consideration, which will be discussed in posterior Sections 3.3 and 3.4. The further increasing of gold loading to 6 wt% induced almost unchanged conversion (98–99%), but the benzaldehyde selectivity was reduced to 95% (benzoic acid selectivity increasing from 1% to ~4%). This is maybe because over high Au-loading (⩾5 wt%) induced overmuch active sites, thereby leading to the overoxidation of benzaldehyde. Among the pre-activated samples, as shown in Fig. 2D, the Au-4/Ni-fiber-300 catalyst calcined at 300 °C delivered the highest benzyl alcohol conversion after pre-activation. Such moderate calcination temperature is likely favorable to the $NiCl_2$-to-NiO transformation and generation of proper Au–NiO interaction (discussed in posterior Section 3.4) on the Au-4/Ni-fiber-300 catalyst compared to the ones calcined at lower (200–250 °C) and higher temperatures (350–400 °C).

Based on above investigation and analysis, the best catalyst was determined as the pre-activated Au-4/Ni-fiber-300 and the highest conversion of ~99% was achieved at 280 °C with a selectivity of ~99%. The by-products including benzene, toluene, benzoic acid, and small amount of CO_x were detected. As a contrastive experiment, neat Ni-fiber supports calcined in air at temperatures ranging from 200 to 600 °C were pre-activated at 380 °C and delivered the highest benzyl alcohol conversion of only 4% with selectivity of 99% under identical reaction conditions. The above results definitely indicated that Au embedment modification of Ni-fiber remarkably enhanced the low-temperature activity. It should be pointed out that, unless otherwise specified, the reaction results reported in the posterior parts are all based on the pre-activated catalyst samples.

3.2.2. Effects of reaction conditions

The effects of reaction conditions (including WHSV, O_2/ol ratio, and reaction temperature) on the performance of Au-4/Ni-fiber-300 catalyst for the gas-phase selective oxidation of benzyl alcohol are shown in Fig. 3.

At 280 °C under a WHSV of 20 h^{-1}, the benzyl alcohol conversion was 77% with O_2/ol ratio of 0.4 (Fig. 3A; stoichiomatric O_2/ol ratio is 0.5), slightly lower than the theoretically attainable conversion of 80% at 100% selectivity to benzaldehyde, indicating that the pre-activated Au-4/Ni-fiber-300 catalyst showed a very high O_2 utilization efficiency (over 96%). With increasing O_2/ol from 0.4 to 0.6 and then up to 1.2, the benzyl alcohol conversion was increased to ~99% and then slowly decreased down to ~95% while the selectivity to benzaldehyde remained almost unchanged. This indicated that excess O_2 showed some suppressing effect on the activity of our Au/Ni-fiber catalysts but not on the selectivity. Such suppressing effect is very interesting, but the reason for it is not clear yet now. On the balance between benzyl alcohol conversion and O_2 utilization efficiency, the optimal O_2/ol ratio was set as 0.6.

As shown in Fig. 3B, with the increase in WHSV from 10 to 40 h^{-1}, the conversion of benzyl alcohol was smoothly increased from 89% to 99% while the selectivity to benzaldehyde decreased from 99% to 95% at 280 °C with an O_2/ol ratio of 0.6. It is likely due to the related increase in real bed temperature (Fig. S4 and detailed explanation). The temperature difference between catalyst bed and reactor external wall (ΔT) was 4 °C at the WHSV of 10 h^{-1} and 18 °C at the WHSV of 40 h^{-1}, respectively. Further increasing WHSV up to 70 h^{-1}, the benzyl alcohol conversion was decreased to 80% but the selectivity was increased from 95% to 99%. Meanwhile, the ΔT was slightly increased from 18 to

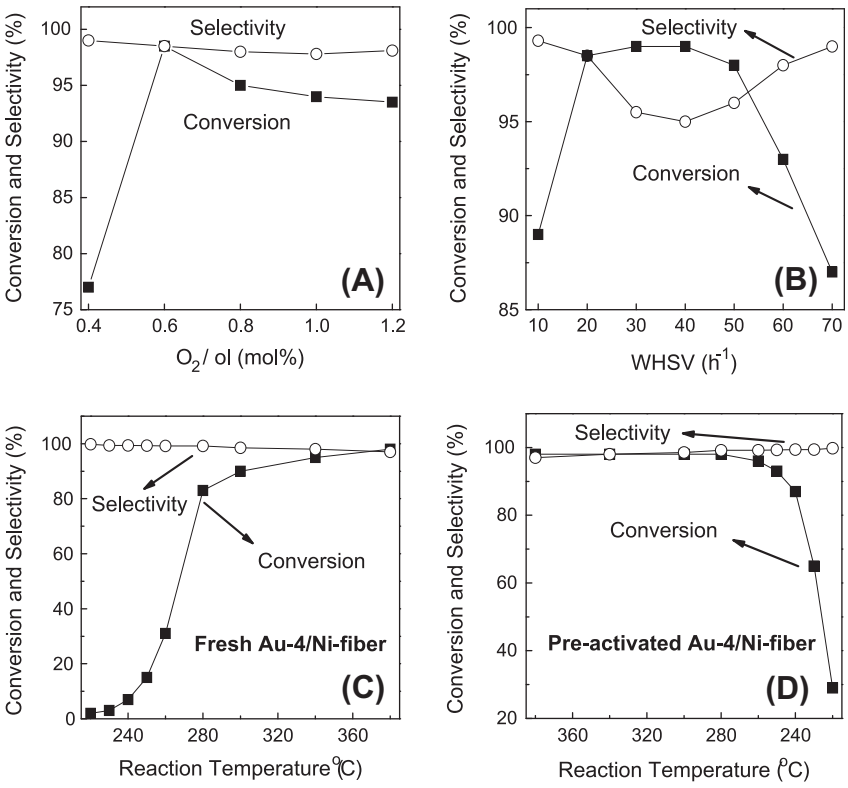

Fig. 3. Effects of the reaction conditions on the catalyst performance. (A) O_2/ol ratio with WHSV = 20 h^{-1} and (B) WHSV with O_2/ol = 0.6 on the pre-activated Au-4/Ni-fiber-300 catalyst for the gas-phase oxidation of benzyl alcohol at 280 °C. Pre-activation conditions: same as in Fig. 2. The conversion and selectivity over the Au-4/Ni-fiber-300 catalyst (C) before pre-activation treatment for the gas-phase oxidation of benzyl alcohol with temperature from 220 °C up to 380 °C, and (D) after pre-activation treatment from 380 °C down to 220 °C using a O_2/ol ratio of 0.6 and WHSV of 20 h^{-1}.

25 °C. Increasing WHSV from 40 to 70 h^{-1}, the residence time was insufficient for more reactant and product molecules to react with O_2 thereby leading to the decrease in conversion (Fig. S4 and detailed explanation). Considering a balance between high product yield and small ΔT, the optimal WHSV was set as 20 h^{-1}.

As shown in Figs. 3C and D, the as-prepared Au-4/Ni-fiber-300 catalyst and the pre-activated catalysts provided quite different conversion profile of the benzyl alcohol oxidation with increasing reaction temperature from 220 to 380 °C, at a constant WHSV of 20 h^{-1} and O_2/ol of 0.6. For the as-prepared catalysts (Fig. 3C), a sudden increase in the benzyl alcohol conversion was observed at around 280 °C. After undergoing the reaction for 1 h at 380 °C (pre-activation), the catalyst was tested again with the decrease in reaction temperature from 380 to 220 °C, with the results as shown in Fig. 3D. In contrast, the conversion almost remained constant (93–98%) until the temperature was reduced to 240 °C while the conversion decreased slightly to 86% and then sharply dropped to 28% at the temperature of 220 °C (15 °C higher than the boiling point of benzyl alcohol). Interestingly, the benzyl alcohol conversion of 93% and benzaldehyde selectivity of 99% could be obtained at 250 °C, which are much better than the previous reports. For example, the highest benzaldehyde yield of only ~42% (conversion: ~53%, selectivity: ~80%) was obtained on the electrolytic silver catalyst even at 500 °C and a low WHSV of 8 h^{-1} [14]. When the silver catalyst supported on the zeolite film coated on copper grid, it just delivered a benzyl alcohol conversion of 57% and selectivity of 90% at 320 °C [13]. Our previously reported Ag/Ni-fiber catalyst could yield comparable conversion (92–95%) and selectivity (95–97%) but only at or above 300 °C [14,15,26].

3.2.3. High heat conductivity

Ni-fiber supported catalysts provide desirable heat conductivity during reaction, which facilitates rapid dissipation of the reaction heat in catalyst bed liberated from such strongly exothermic oxidation process. It could reduce the catalyst degradation and surface hotspots and, consequently, increase the catalyst lifetime. As shown in Fig. 4, the catalytic bed packed with Au/Ni-fiber delivered a very low ΔT of 6 °C between catalyst bed and reactor external wall in the oxidation of benzyl alcohol at 250 °C, and 9 °C at 280 °C with a WHSV of 20 h^{-1}, which is much lower than that on the oxide-supported catalysts [16–18]. A ΔT of 56 °C was observed for the oxidation of benzyl alcohol on Au–Cu/SiO_2 at the WHSV of 10 h^{-1} [17], and ~17 °C on K–Cu–TiO_2 even under an extremely

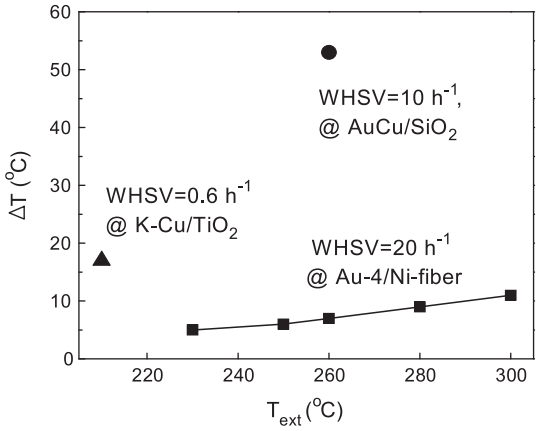

Fig. 4. Temperature difference (ΔT) between the set-up temperature (T_{ext}) and the catalyst bed temperature (T_{bed}) in the gas-phase oxidation of benzyl alcohol over the pre-activated Au-4/Ni-fiber-300, Au–Cu/SiO_2 [17], and K–Cu–TiO_2 [18]. Pre-activation: same as in Fig. 2.

low WHSV of 0.6 h^{-1} [18]. It should be noted that the heat-liberating rates over the Au–Cu/SiO_2 and K–Cu–TiO_2 are 50%, and only 3% of Au-4/Ni-fiber-300 in our work using WHSV of 20 h^{-1}, consuming at equivalent alcohol conversion (>95%) and product selectivity (>97%).

3.2.4. Oxidation for other alcohols

The pre-activated Au-4/Ni-fiber-300 was also tested for the oxidation of a range of straight-chain, benzylic, and polynary (1,2-propanediol) alcohols. The results showed that the catalytic performance was influenced by the structure of alcohol substrates (Table 1). The faster oxidation of conjugated aromatic alcohols to the corresponding conjugated aldehydes or ketones was observed compared to the oxidation of aliphatic alcohols. The pre-activated Au-4/Ni-fiber-300 could selectively oxidize 1-phenylethanol to acetophenone at a high conversion of 99% at 300 °C but only converted 49% of 2-phenylethanol even at higher temperature of 340 °C. For octanol, the primary linear aliphatic alcohol (1-ol) was more active than the secondary counterparts (2-ol) during the oxidation, in good agreement with the previous work [41]. Interestingly, cyclohexanol and cyclopropyl carbinol were very reactive among the aliphatic alcohols. Cyclohexanol was selectively oxidized to cyclohexanone at a conversion of 73% with the selectivity of 99% at 340 °C. Cyclohexanone is a key raw material in synthesis of many useful chemicals, such as caprolactam fornylon 6 and adipic acid for nylon 66. In the case of cyclopropyl carbinol, the conversion of 92% was obtained at 280 °C with 97% selectivity to cycloprogyl dehyde, which is an important synthetic building block and a new-type bactericide. Furthermore, alcohols containing two hydroxyl groups, such as 1,2-propylene glycol which is favorable to form hydroxylketone rather than methyl glyoxal, could also be oxidized to the target product (methyl glyoxal) with the selectivity of 66% at the conversion of 99%.

3.2.5. Stability

One challenge for heterogeneous catalysts is their stability. As shown in Fig. S5, the stability of the pre-activated Au-4/Ni-fiber-300 was investigated during the oxidation of benzyl alcohol in a single-run lifetime of 140 h at 280 °C under a steady catalytic reactivity (conversion: 94–99%; selectivity: 99%). When decreasing the reaction temperature to 250 °C, the single-run lifetime could be extended to 230 h with a slight conversion loss of <5%. The spent catalyst was regenerated after calcining in air at 380 °C to burn off the deposited carbon (6.4 wt% of carbon per gram catalyst after a 230-h run at 250 °C; determined by weighing the catalyst before and after reaction). The pre-activated Au-4/Ni-fiber-300 catalyst remained its high activity (selectivity > 99%) after twice regenerations (660-h time-on-stream, Fig. 5), thus showing promising stability. A high product yield of benzaldehyde

Table 1
Oxidation of various alcohols over the pre-activated Au-4/Ni-fiber-300 catalyst.

Substrate	O_2/ol ratio (mol/mol)	Reaction temperature (°C)	Conversion (%)	Selectivity (%)
1-Phenylethanol	0.8	300	99	97
2-Phenylethanol	0.8	340	49	99
1-Octanol	0.6	300	57	90
2-Octanol	0.6	380	26	64
Cyclohexanol	0.6	340	73	99
Cyclopropyl carbinol	0.6	280	92	97
1,2-Propanediol	1.6	380	99	66

The catalyst was pre-activated (i.e., undergoing gas-phase selective oxidation of benzyl alcohol at 380 °C for 1 h using O_2/ol = 0.6 and WHSV = 20 h^{-1}) and then evaluated at the specified temperature using WHSV = 20 h^{-1}.

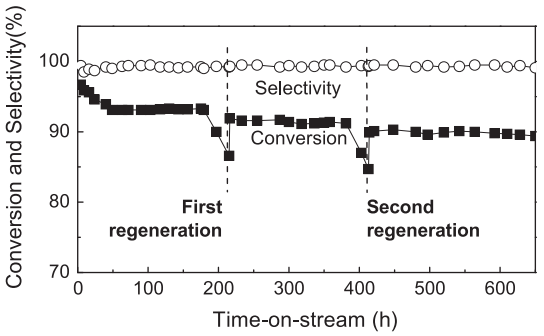

Fig. 5. Lifetime test of the pre-activated Au-4/Ni-fiber-300 catalyst. Reaction conditions: O_2/ol = 0.6, WHSV = 20 h^{-1}, T = 250 °C. Pre-activation: same as in Fig. 2.

(10 kg per gram Au-4/Ni-fiber-300 or 250 kg per gram Au) was achieved after this 660-h run. Moreover, the liquid effluent was automatically separated into water phase and clear pale yellow organic phase wherein benzaldehyde was dominant (benzene, toluene, and benzoic acid were formed only in traces). In the first 215-h lifetime test of the Au-4/Ni-fiber-300 catalyst, 1.23 kg of benzyl alcohol was consumed. The average benzyl alcohol conversion and benzaldehyde selectivity was 93.1% and 99.2%, respectively, and the selectivity of 0.8% was contributed to benzene (0.003%), toluene (0.047%), and benzoic acid (0.75%). The ideal and actual mass of the product based on the above conversion and selectivity was 1387 and 1384 g, respectively, and therefore, a very high mass balance of ~99.8% was achieved.

3.3. Insensitiveness of gold particle size

The results presented in this work show that the pre-activated Au-4/Ni-fiber-300 with 25 nm Au particles (estimated from the Scherrer equation according to Au(1 1 1) XRD peak in Fig. S6) was very efficient for the low-temperature gas-phase oxidation of several typical alcohols. However, the gold particles with the size smaller than 5 nm, especially in the range of 2–3 nm was primarily considered to have acceptable catalytic activity [45,46]. Recently, several gold catalysts with big particle size have also been reported to be active in some reaction processes [16,17,47], but the detailed catalysis nature remains unrevealed yet. In this work, the catalysis origin of our Au/Ni-fiber catalyst would be explored.

Fig. 6 shows the XRD patterns of the pre-activated catalysts with different gold loadings (1–5 wt%). The gold particle sizes of

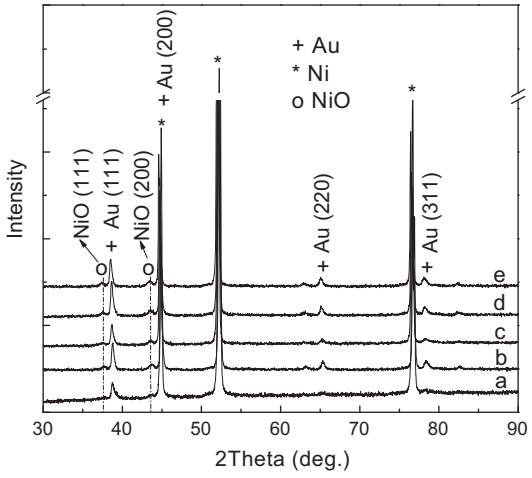

Fig. 6. XRD patterns of the pre-activated catalysts with different gold loadings of (a) 1 wt%, (b) 2 wt%, (c) 3 wt%, (d) 4 wt%, and (e) 5 wt%. Reaction and pre-activation conditions: same as in Fig. 2.

Table 2
The gold particle size, benzyl alcohol conversion, and turnover frequencies (TOFs) of the pre-activated catalysts with different gold loadings (1–5 wt%).[a]

Catalyst	Au-loading (wt%)	D_{Au}[b] (nm)	Conv. (%)	Sel. (%)	TOF (h^{-1})[c]
Au-1/Ni-fiber-300	1	19	14	100	7705
Au-2/Ni-fiber-300	2	23	77	99	25,294
Au-3/Ni-fiber-300	3	24	90	99	20,758
Au-4/Ni-fiber-300	4	25	98	99	17,634
Au-5/Ni-fiber-300	5	28	97	99	15,217

[a] The catalysts were pre-activated (i.e., undergoing gas-phase selective oxidation of benzyl alcohol at 380 °C for 1 h using O_2/ol = 0.6 and WHSV = 20 h^{-1}) and then evaluated at 280 °C using WHSV of 20 h^{-1} and O_2/ol of 0.6.
[b] The particle size was estimated from XRD patterns using Scherrer equation.
[c] TOF was calculated based on the surface amount of Au atoms present in the samples (see Table S1 in Supporting information).

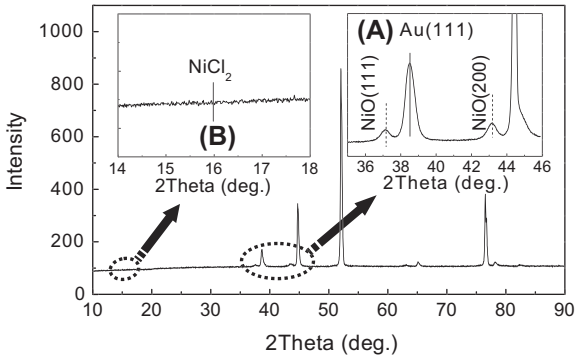

Fig. 7. XRD patterns of the pre-activated Au-4/Ni-fiber-300 catalyst. (A) The formation of NiO (2θ = 37.4° and 43.4°); (B) the disappearance of $NiCl_2$ (2θ = 16°). Pre-activation: same as in Fig. 2.

the pre-activated Au/Ni-fiber-300 catalysts calculated from the Scherrer equation according to Au(111) XRD peak in Fig. 6, the conversion for the gas-phase oxidation of benzyl alcohol on the catalysts in Fig. 2C, and the corresponding turnover frequency (TOF) are summarized in Tables 2 and S1. Increasing the Au-loading from 1 to 5 wt%, the gold particle size increased from 19 to 28 nm. The benzyl alcohol conversion on these catalysts was sharply promoted from 14% to 77% with increasing the Au-loading from 1 to 2 wt% and then was smoothly increased from 90% to 98% with increasing the Au-loading up to 5 wt%. Take the Au-1/Ni-fiber-300 and Au-2/Ni-fiber-300 catalysts for comparison of the intrinsic activity by their TOFs. Although the Au-1/Ni-fiber-300 had a smaller gold average particle size than that of Au-2/Ni-fiber-300, its TOF was much lower than that of Au-2/Ni-fiber-300. Similarly, the Au-(3–5)/Ni-fiber-300 catalysts with large gold particle size (24–28 nm) were also more active than the Au-1/Ni-fiber-300 catalyst with gold particle size of 19 nm: TOF of 15,217–20,758 h^{-1} vs. TOF of 7705 h^{-1}. Therefore, it seemed that the gold particle size is not crucial for the activity of our Au/Ni-fiber catalysts in the gas-phase oxidation of alcohols.

3.4. Transformation of $NiCl_2$ to NiO for low-temperature activity

It should be noted that the activity of Au-4/Ni-fiber-300 catalyst was enhanced dramatically after the pre-activation process at 380 °C, but this phenomena did not occur even after a longer (e.g., 6 h) time-on-stream at temperatures below 250 °C (Fig. S7). It is expected that the pre-activation has changed the surface morphology and nanostructure/composition of the catalysts.

The HRTEM images showed that the most gold particles size over the Au-4/Ni-fiber-300 catalyst was very large and almost unchanged after pre-activation (Fig. S8). However, the SEM images clearly showed the surface reconstruction of the $NiCl_2$@Au composites on the as-prepared Au-4/Ni-fiber-300 catalyst after pre-activation (Fig. S9). This was supported by the fact that Cl^- ions were detectable by $AgNO_3$ test rather than the Ni^{2+} ions by ICP in the initial liquid effluent during the pre-activation. Furthermore, it is clear from XRD and XPS analyses that complete transformation from $NiCl_2$ to NiO occurred and surface Au/Ni atom ratio was determined to be 1/35 on the Au-4/Ni-fiber-300 after pre-activation (Fig. 7, Figs. S10 and S11 and detailed discussion). In addition, such transformation was also clearly observed by XRD patterns of other catalysts except the one with 1 wt% Au (Fig. S12). By combining this observation with the results as shown in Fig. 2C, it indicated that the catalytic behavior of catalysts along with their Au-loadings correlated very well with the formation of NiO NPs (Figs. 6 and S12). When the as-prepared Au-4/Ni-fiber-300 was washed thoroughly using deionized water just after galvanic exchange reaction followed by calcination at 300 °C (the resulting catalyst was denoted as Au-4/Ni-fiber-W-300), the benzyl alcohol conversion on this catalyst was decreased from ~99% to 39%. Since most of $NiCl_2$ formed during galvanic deposition was removed from the surface, no apparent NiO NPs was formed from $NiCl_2$ during the pre-activation process (Fig. 8).

However, a question attacked us whether the NiO NPs play an essential role in contributing the low-temperature activity. To address this question, a contrastive catalyst of NiO-3/Ni-fiber was

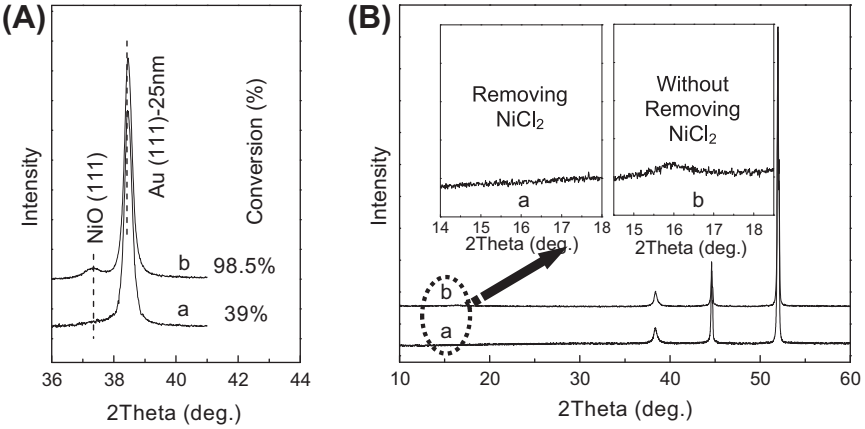

Fig. 8. XRD patterns of (A) the pre-activated and (B) the as-prepared catalysts. (A-a) Pre-activated Au-4/Ni-fiber-W-300 with the absence of NiO (2θ = 37.3°); (A-b) pre-activated Au-4/Ni-fiber-300; (B-a) as-prepared Au-4/Ni-fiber-W-300; (B-b) as-prepared Au-4/Ni-fiber-300. Insert-a: showing no $NiCl_2$ peak at 2θ = 16°; Insert-b: showing the $NiCl_2$ peak at 2θ = 16°). Pre-activation conditions: same as in Fig. 2. *Note*: Au-4/Ni-fiber-W-300 catalyst, with removal of formed $NiCl_2$, was obtained by thoroughly washing the catalyst just after galvanic deposition using deionized water before drying and calcining at 300 °C in air.

prepared by impregnating Ni-fiber with $Ni(NO_3)_2$ solution (to 3 wt% NiO), drying at 80 °C overnight, and calcining at 300 °C. The benzyl alcohol conversion was only 5% at 280 °C over NiO-3/Ni-fiber. In order to further address this question, two more contrastive catalysts, NiO-3/Ti-fiber and Au-4/Ti-fiber, were prepared by the same method as for the NiO-3/Ni-fiber catalyst except using Ti-fiber as support, yielding the benzyl alcohol conversion of less than 10%. Interestingly, the Au-4/Ti-fiber catalyst after re-impregnation with $Ni(NO_3)_2$ solution (to 3 wt% NiO) followed by calcination at 300 °C, yielded a sharp promotion of the benzyl alcohol conversion up to 94% at 280 °C. These results obviously indicated that the Au–NiO composites play an essential role in contributing the activity for alcohol oxidation, which is consistent with the reported Au catalysts supported on NiO for CO [39] and alcohol oxidation [48]. One can thus say that the pre-activation process over the Au/Ni-fiber catalyst by nature facilitated the $NiCl_2$-to-NiO transformation to form the Au–NiO composites, which led sharp promotion of the catalyst activity for alcohol oxidation.

4. Conclusions

The high-performance gold on Ni-fiber catalysts, which showed a unique combination of excellent low-temperature activity, high selectivity, good stability and high heat-transfer ability, were successfully prepared for the low-temperature gas-phase selective oxidation of various alcohols. The Au/Ni-fiber catalysts were obtained by galvanic deposition of Au onto a thin-sheet microfibrous structure consisting of 5 vol.% 8-μm Ni-fiber and 95 vol.% voidage. The best catalyst was Au-4/Ni-fiber-300 (Au-loading: 4 wt%; calcined at 300 °C in air), which was effective for acyclic, benzylic, and polynary (1,2-propanediol) alcohols using a high WHSV of 20 h^{-1}. For benzyl alcohol, the conversion of ~95% was achieved and retained with >98% selectivity to benzaldehyde in a 660 h test at 250 °C. The spent catalyst can be recovered to its as-prepared one exhibiting comparable activity/selectivity by a simple heating treatment in air. A low ΔT of <10 °C between the catalyst bed and reactor external wall was observed in the selective oxidation of benzyl alcohol, owing to the enhanced heat-transfer ability that permits to rapidly dissipate large quantities of reaction heat. A significant promotion of the low-temperature activity of the Au-4/Ni-fiber-300 catalyst took place, which is attributed to the transformation of $NiCl_2$ (formed at Au galvanic deposition step) into NiO NPs around Au particles. The pre-activation process (e.g., pre-reaction at a high temperature of 380 °C for 1 h) facilitated the $NiCl_2$-to-NiO transformation. Despite these interesting results, in-depth investigation of the interaction between NiO and Au particles with respect to NiO–Au nano-architecture, nature of the synergistic effect, and active site structure is particularly desirable.

Acknowledgments

This work was funded by the NSF of China (21273075, 21076083, 20973063), the "973 program" (2011CB201403) from the MOST of China, the Fundamental Research Funds for the Central Universities, the Shanghai Rising-Star Program (10HQ1400800), the Specialized Research Fund for the Doctoral Program of Higher Education (20090076110006), and the Shanghai Leading Academic Discipline Project (B409). We thank the Electron Spectroscope Center of the East China Normal University for assistance with TEM measurements.

Appendix A. Supplementary material

Supplementary data associated with this article can be found, in the online version, at http://dx.doi.org/10.1016/j.jcat.2013.01.020.

References

[1] R.A Sheldon, J.K Kochi, Metal-Catalyzed Oxidations of Organic Compounds, Academic Press, New York, 1981.
[2] T. Mallat, A. Baiker, Chem. Rev. 104 (2004) 3037.
[3] A.S.K. Hashmi, Chem. Rev. 107 (2007) 3180.
[4] A. Corma, H. Garcia, Chem. Soc. Rev. 37 (2008) 2096.
[5] J.I. Kroschwitz, Kirk Othmer Encyclopedia of Chemical Technology, vol. 4, fourth ed., Wiley-Interscience Publications, New York, 1992, pp. 64–72.
[6] D.G. Lee, U.A. Spitzer, J. Org. Chem. 35 (1970) 3589.
[7] F.M. Menger, C. Lee, Tetrahedron Lett. 22 (1981) 1655.
[8] G. Cainelli, G. Cardillo, Chromium Oxidants in Organic Chemistry, Springer, Berlin, 1984.
[9] U.R. Pillai, E. Sahle-Demessie, Appl. Catal. A 245 (2003) 103.
[10] R.A. Sheldon, M. Wallau, I.W.C.E. Arends, U. Schuchardt, Acc. Chem. Res. 31 (1998) 485.
[11] G.J.T. Brink, I.W.C.E. Arends, R.A. Sheldon, Science 287 (2000) 1636.
[12] H. Tsunoyama, H. Sakurai, Y. Negishi, T. Tsukuda, J. Am. Chem. Soc. 127 (2005) 9374.
[13] J. Shen, W. Shan, Y. Zhang, J. Du, H. Xu, K. Fan, W. Shen, Y. Tang, J. Catal. 237 (2006) 94.
[14] J.P. Mao, M.M. Deng, Q.S. Xue, L. Chen, Y. Lu, Catal. Commun. 10 (2009) 1376.
[15] J.P. Mao, M.M. Deng, L. Chen, Y. Liu, Y. Lu, AIChE J. 56 (2010) 1545.
[16] S. Biella, M. Rossi, Chem. Commun. (2003) 378.
[17] C.D. Pina, E. Falleta, M. Rossi, J. Catal. 260 (2008) 384.
[18] J. Fan, Y.H. Dai, Y.L. Li, N.F. Zheng, J.F. Guo, X.Q. Yan, G.D. Stucky, J. Am. Chem. Soc. 131 (2009) 15568.
[19] H. Hayashibara, S. Nishiyama, S. Tsuruya, M. Masai, J. Catal. 153 (1995) 254.
[20] R. Yamamoto, Y. Sawayama, H. Shibahara, Y. Ichihashi, S. Nishiyama, S. Tsuruya, J. Catal. 234 (2005) 308.
[21] D.K. Harris, D.R. Cahela, B.J. Tatarchuk, Compos. Part A: Appl. Sci. Manuf. 32 (2001) 1117.
[22] Y. Liu, H. Wang, J.F. Li, Y. Lu, Q.S. Xue, J.C. Chen, AIChE J. 53 (2007) 1845.
[23] Y. Lu, H. Wang, Y. Liu, Q.S. Xue, L. Chen, M.Y. He, Lab Chip 7 (2007) 133.
[24] M.M. Wang, J.F. Li, L. Chen, Y. Lu, Int. J. Hydrogen Energy 34 (2009) 1710.
[25] M. Lin, G.F. Zhao, W. Chen, M.M. Wang, Q.S. Xue, Y. Lu, Int. J. Hydrogen Energy 36 (2011) 12833.
[26] M.M. Deng, G.F. Zhao, Q.S. Xue, L. Chen, Y. Lu, Appl. Catal. B 99 (2010) 222.
[27] G.F. Zhao, H.Y. Hu, M.M. Deng, M. Ling, Y. Lu, Green Chem. 13 (2011) 55.
[28] B.K. Chang, Y. Lu, B.J. Tatarchuk, Chem. Eng. J. 115 (2006) 195.
[29] R.R. Kalluri, D.R. Cahela, B.J. Tatarchuk, Appl. Catal. B 90 (2009) 507.
[30] W. Chen, W.Q. Sheng, G.F. Zhao, F.H. Cao, Q.S. Xue, L. Chen, Y. Lu, Int. J. Hydrogen Energy 37 (2012) 18021.
[31] W. Chen, W.Q. Sheng, G.F. Zhao, F.H. Cao, Q.S. Xue, L. Chen, Y. Lu, RSC Adv. 2 (2012) 3651.
[32] G.F. Zhao, H.Y. Hu, M.M. Deng, M. Ling, Y. Lu, ChemCatChem 3 (2011) 1629.
[33] G.F. Zhao, H.Y. Hu, M.M. Deng, Y. Lu, Chem. Commun. 47 (2011) 9642.
[34] J. Chen, B. Wiley, Z.-Y. Li, D. Campbell, F. Saeki, H. Cang, L. Au, J. Lee, X. Li, Y. Xia, Adv. Mater. 17 (2005) 2255.
[35] H. Zhang, T. Watanabe, M. Okumura, M. Haruta, N. Toshima, Nat. Chem. 11 (2012) 49.
[36] A. Davidson, J.F. Tempere, M. Che, H. Roulet, G. Dufour, J. Phys. Chem. 100 (1996) 4919.
[37] Q. Fu, H. Saltsburg, M. Flytzani-Stephanopoulos, Science 301 (2003) 935.
[38] A. Abad, P. Concepcion, A. Corma, H. Garcia, Angew. Chem. Int. Ed. 44 (2005) 4066.
[39] M. Haruta, N. Yamada, T. Kobayashi, S. Iijima, J. Catal. 115 (1989) 301.
[40] J.D. Grunwaldt, M. Maciejewski, O.S. Becker, P. Fabrizioli, A. Baiker, J. Catal. 186 (1999) 458.
[41] D.I. Enache, J.K. Edwards, P. Landon, B. Solsna-Espriu, A.F. Carely, A.A. Herzing, M. Watanabe, C.J. Kiely, D.W. Knight, G.J. Hutchings, Science 311 (2006) 362.
[42] A.S.K. Hashmi, G.J. Hutchings, Angew. Chem. Int. Ed. 45 (2006) 7896.
[43] H. Miyamura, R. Matsubara, Y. Miyazaki, S. Kabayashi, Angew. Chem. Int. Ed. 46 (2007) 4151.
[44] F.Z. Su, Y.M. Liu, L.C. Wang, Y. Cao, H.Y. He, K.N. Fan, Angew. Chem. Int. Ed. 47 (2008) 334.
[45] M.S. Chen, D.G. Goodman, Science 306 (2004) 252.
[46] B.K. Min, C.M. Friend, Chem. Rev. 107 (2007) 2709.
[47] B. Zhu, M. Lazar, B.G. Trewyna, R.J. Angelici, J. Catal. 260 (2008) 1.
[48] A. Villa, G.M. Veith, D. Ferri, A. Weidenkaff, K.A. Perry, S. Campisia, L. Prati, Catal. Sci. Technol. 3 (2013) 394.